Establishment of *in vitro* three-dimensional cementocyte differentiation scaffolds to study orthodontic root resorption

TINGTING WEI[1], YUFEI XIE[2], XIN WEN[3], NING ZHAO[3] and GANG SHEN[3]

[1]Department of Orthodontics, Shanghai Key Laboratory of Stomatology, Ninth People's Hospital, College of Stomatology, Shanghai Jiao Tong University School of Medicine, Shanghai 200011; [2]Department of Orthodontics, Shanghai Xuhui District Dental Disease Prevention and Control Institute, Shanghai 200001; [3]Department of Orthodontics, Ninth People's Hospital, College of Stomatology, Shanghai Jiao Tong University School of Medicine, Shanghai 200011, P.R. China

Received January 15, 2020; Accepted May 28, 2020

DOI: 10.3892/etm.2020.9074

Abstract. Orthodontic-induced root resorption is a severe side effect that can lead to tooth root shortening and loss. Compressive force induces tissue stress in the cementum that covers the tooth root, which is associated with activation of bone metabolism and cementum resorption. To investigate the role of cementocytes in mechanotransduction and osteoclast differentiation, the present study established an *in vitro* three-dimensional (3D) model replicating cellular cementum and observed the effects of static compression on the cellular behavior of the cementocytes. Cell Counting Kit-8 assay, alkaline phosphatase staining and dentin matrix protein 1 quantification were used to evaluate the cementocyte differentiation in the 3D scaffolds. Cellular viability under static compression was evaluated using live/dead staining, and expression of mineral metabolism-related genes were analyzed via reverse transcription-quantitative PCR. The results suggested that the cementocytes maintained their phenotype and increased the expression of osteoprotegerin (OPG), receptor activator of NF-κB ligand (RANKL) and sclerostin (SOST) in the 3D model compared with cells cultured in two dimensions. Compression force increased cell death and induced osteoclastic differentiation via the upregulation of SOST and RANKL/OPG ratio, and the downregulation of osteocalcin. The effect of compression showed a force magnitude-dependent pattern. The present study established an *in vitro* model of cellular cementum to study the biology of cementocytes. The results indicated that cementocytes are sensitive to mechanical loading and may serve potential roles in the metabolic regulation of minerals during orthodontic root resorption. These findings provide a novel tool to study biological processes in the field of orthodontics and expand knowledge of the biological function of cementocytes.

Correspondence to: Dr Gang Shen, Department of Orthodontics, Ninth People's Hospital, College of Stomatology, Shanghai Jiao Tong University School of Medicine, 500 Quxi Road, Shanghai 200011, P.R. China
E-mail: shengang@bybo.com.cn

Key words: cementocytes, cementum, orthodontic tooth movement, three-dimensional cell culture, mechanical loading

Introduction

Cementocytes are the cellular components of cementum. The cementum, which is the thin mineral layer lining the dental root and connecting the periodontal ligaments (PDLs), functions as the anchor of the teeth to the PDLs and as a regulator of tooth position (1). Loss of cementum leads to periodontal disorder and tooth displacement and loss (2). It has been previously reported that 48-66% of roots suffer resorption of cementum after orthodontic treatment, indicating the susceptibility of the cementum to orthodontic force (3). Although the root's outermost layer, the cellular cementum, which is also known as cellular intrinsic fiber cementum, is considered to exhibit a general protective function against resorption, the response and function of cementocytes are largely unknown (4).

The limited understanding of the regulatory role of cementocytes under orthodontic stimulation is attributed to: i) *In vitro* difficulties in accessing and characterizing the cementocytes, which are terminally differentiated cells, and are embedded with hard dental roots in small quantities; ii) lack of immortalized cell lines that resemble the phenotypic features of non-proliferating mature cementocytes (5,6); iii) technical challenges in establishing an *in vitro* stress loading model to replicate the orthodontic force on the cementum, using regular two-dimensional (2D) monolayer cultured cells (7-9).

To improve the understanding of cementocytes, the cementocyte cell line IDG-CM6 has been established, and efforts have been made to generate an *in vitro* analysis system (6). Force types, such as cyclic tensile and intermittent compression forces, have been used to analyze cementoblasts and periodontal cells (10,11). However, the results of these systems are variable, and the association of these systems with *in vivo* mechanical loading requires additional elucidation. The majority of the stress loading models, which have been developed *in vitro* to study cellular mechanotransduction (11-17), are based on cells cultured in 2D monolayer

disks or flasks, which lack the characteristics of the natural tissue microenvironment (11,14,16,17). Previous studies have indicated that three-dimensional (3D) cultures can induce differentiation of osteoblasts (18), simulate the *in vivo* differentiation pathway (19) and replicate a more realistic tissue microenvironment where cells may be subjected to mechanical loading (8). 3D cell models are mostly assembled by gels or scaffolds (13,20-23), both of which can imitate the *in vivo* spatial structure, and demonstrate the features of cells subjected to mechanical forces. Due to their elasticity, collagen gels are widely used as supports and as a transfer of direct compressive force (15,24-26). These 3D culture models are principally used to study differentiation and mineralization of osteoblasts and osteocytes. However, 3D culture models for *ex vivo* investigation of cementocytes have not been reported to date, to the best of our best knowledge.

The principal aims of the current study were to establish an *in vitro* 3D stress loading model replicating orthodontic force on cementocytes and investigate the response of cementocytes to continuous compressive force of varying magnitude, via evaluating the expression of the biomarkers involved in cementum remodeling.

Materials and methods

2D cell culture. The murine cementocyte-like cell line IDG-CM6 was kindly provided by Professor Lynda F. Bonewald (Indiana University, Indianapolis, USA) and used in the experiments after mycoplasma testing using a mycoplasma detection kit (Beijing Solarbio Science & Technology Co., Ltd.) (6). This murine cell line was derived from the cementum of Immortomouse/dentin matrix protein 1 (DMP1)-green fluorescent protein $(GFP)^{+/-}$ mice, and the immortalization was mediated via interferon-gamma (IFN-γ) to express a thermolabile large T antigen, as previously described (6). Cells within passages 5-15 were thawed at 33˚C and resuspended in α-minimum essential medium (α-MEM) with L-glutamine and nucleosides (HyClone; Cytiva), supplemented with 10% FBS (Gibco; Thermo Fisher Scientific, Inc.), 100 U/ml penicillin and 100 µg/ml streptomycin. Recombinant mouse IFN-γ (50 U/ml; Thermo Fisher Scientific, Inc.) was also added in the proliferation medium. Cells were then distributed on collagen-coated dishes (rat tail type I collagen at a concentration of 0.15 mg/ml in 0.02 M acetic acid; Corning Inc.) and incubated at 33˚C with 5% CO_2 for 24 h. At 80-90% confluency, cells were sub-cultured with 0.05% trypsin/0.53 mM EDTA solution (Gibco; Thermo Fisher Scientific, Inc.) at 33˚C for 2 min.

3D cell culture system. The 3D culture system was based on a protocol described previously (27), which was slightly modified. The cells were resuspended in α-MEM and added to the hydrogel mixture on ice. The constructs comprised 5% FBS (Gibco; Thermo Fisher Scientific, Inc.), 10% 5X αMEM (Gibco; Thermo Fisher Scientific, Inc.), 20% Matrigel (8-12 mg/ml; Corning Inc.), 40% rat tail type I collagen (3.79-4.10 mg/ml; Corning Inc.) and 25% cell suspension (1-2x10^6 cells/ml), and were neutralized with 1M sodium hydroxide (Merck KGaA). 500 µl of the mixture were distributed per well in a 24-well plate. The plate was subsequently incubated at 37˚C for 1 h for gel polymerization. The proliferation medium was α-MEM supplemented with L-glutamine and nucleosides, 10% FBS, penicillin (100 U/ml) and streptomycin (100 µg/ml) and recombinant mouse IFN-γ (50 U/ml). The cell constructs were cultured at 33˚C with 5% CO_2 for 24 h.

Cell osteogenic differentiation. The overexpression of the thermolabile large T antigen, which is a technique widely used in cell line immortalization, induces cell division in immortalized cells (28). In a previous study, in the case of the IDG-CM6 cell line, T antigen was expressed at 33˚C, which induced cell division, but the level of T antigen was decreased after culture of the cells for 24 h at 37˚C. In the absence of T antigen, the cells better resemble the mature cementocytes in the osteogenic condition (6). To induce cementocyte-like differentiation, IDG-CM6 cells in 2D and 3D cultures were incubated at 37˚C with 5% CO_2 for 0-35 days. The first day incubated at 37˚C was called day 0. The growth medium was replaced by differentiation medium comprising α-MEM containing 10% FBS, 50 mg/ml ascorbic acid (Merck KGaA), 4 mM β-glycerophosphate (Merck KGaA), penicillin (100 U/ml) and streptomycin (100 µg/ml). The cells were observed by light microscopy (Zeiss GmbH) at x200 magnification every 2-3 days.

Proliferation assay. The cell proliferation of IDG-CM6 cells under differentiation conditions was assessed via Cell Counting Kit-8 (CCK-8) assay (Shanghai Yeasen Biotechnology Co., Ltd.) according to the manufacturer's recommendations. In brief, cells were cultured in the aforementioned 3D culture system and differentiation conditions for 0, 3, 7, 10, 14, 21 and 35 days. The cells at each time point were incubated with CCK-8 solution for 2 h at 37˚C, and the absorbance at a wavelength of 450 nm was measured. The aforementioned IDG-CM6 cells differentiated on conventional monolayer dishes (2D) at each time point were used as the control group.

Alkaline phosphatase (ALP) staining and ALP activity assay. 5-Bromo-4-chloro-3-indolyl-phosphate/nitro blue tetrazolium (BCIP/NBT) Color Development kit (Beyotime Institute of Biotechnology) was used for ALP staining according to the manufacturer's instructions. The 3D and 2D cultured cells were seeded in 24-well-plates at a density of 2x10^5 cells/well in differentiation medium at 37˚C with 5% CO_2 for 0, 5, 7, 10, 14 and 21 days. Subsequently, cells were fixed with 4% paraformaldehyde for 10 min at room temperature. After washing twice with ice-cold PBS, the cells were stained with BCIP/NBT for 45 min at room temperature prior to observation under a scanner (Canon, Inc.).

For the ALP activity assay, 3D and 2D cultured cells were incubated in 24-well-plates at a density of 2x10^5 cells/well in differentiation medium at 37˚C with 5% CO_2. After 0, 5, 7, 10, 14 and 21 days of incubation, cells were washed twice with PBS and were lysed on ice for 20 sec in 450 µl ALP buffer with 0.2% TritonX-100 (Beijing Solarbio Science & Technology Co., Ltd.), followed by two freeze-thaw cycles, and the total protein level was subsequently quantified using a BCA kit (Thermo Fisher Scientific, Inc.). A total of 100 µl p-nitrophenyl phosphate (pNPP; Merck KGaA) was added to the same volume of cell lysate, and incubated at 37˚C for

30 min. The absorbance at 405 nm was read in triplicate, and ALP activity was normalized to the total protein level and expressed as μmol pNPP produced per min/mg protein.

GFP expression. The IDG-CM6 cell line is derived from Immortomouse/DMP1-GFP$^{+/-}$ mice, which dispose a DMP1-cis-regulatory system driving DMP1-induced GFP expression (29). Therefore, using IDG-CM6 cells derived from DMP1-GFP$^{+/-}$ mice allowed the identification of DMP1-expressing cells via monitoring the expression of GFP. For the observation of DMP1-GFP, the green fluorescent signal was examined on days 3, 7, 14, 21 and 35 via fluorescence microscopy at x40 magnification (Olympus Corporation). For quantification purposes, 3D and 2D cultured IDG-CM6 cells were incubated in 24-well plates at a density of 2x10^5 cells/well in differentiation medium at 37˚C with 5% CO_2. After 0, 7, 14, 21, 28 and 35 days of differentiation, cells were lysed with RIPA buffer (Beijing Solarbio Science & Technology Co., Ltd.) on ice and centrifuged at 12,000 x g for 10 min at 4˚C. The fluorescence intensity of 100 μl cell lysates was measured with an Infinite® 200 fluorescence plate reader (96-well) at an excitation of 460 nm and an emission of 508 nm (Tecan Group, Ltd). The relative fluorescence units were normalized to the total protein concentration quantified by the BCA assay, as previously described (6).

Static compressive loading. The 3D cultured gel with a density of 2x10^5 cells/gel was transferred to a 12-well plate with differentiation medium after the size of the gel was measured (Fig. 1). The gels were 137±17 mm in diameter and 1.71±0.08 mm in thickness. Sterilized stainless-steel beads were weighed and placed in a sterilized plastic cylinder. The beads and cylinder were placed onto the gels, using the gravity to replicate the static compression applied to the cells. The pressure loaded on the gel was calculated and adjusted to 2, 4, 6 and 8 g/cm^2 using the following formula: $P=4m/\pi d^2$ (m, total weight of the beads and cylinder; d, diameter). Previous studies have reported cell response to compressive loading ranging from 1-24 h (11,19). A total of 8 g/cm^2 of force was applied on the 3D cultured gel for 2-24 h in the preliminary test. It was found that within 6 h, the cell viability did not significantly decrease, but increasing cell death was detected thereafter. Thus, a 6 h duration was used for subsequent tests. During the compression, the cells were incubated at 37˚C with 5% CO_2.

Cell viability assay. LIVE/DEAD™ Viability/Cytotoxicity kit (Thermo Fisher Scientific, Inc.) was used for evaluating cell viability according to the manufacturer's protocol. A solution of 2 μM calcein acetoxymethyl (calcein AM) and 4 μM ethidium homodimer (EthD-1) was added to the gel sample, and subsequently incubated for 30 min at room temperature. Calcein AM is retained in live cells generating green fluorescence, whereas EthD-1 generates red fluorescence in dead cells (30). At least five separate fields at x200 magnification were captured with a fluorescence microscope (Olympus Corporation). Positive cells were counted in each field using ImageJ v1.52 software (National Institutes of Health). Cell viability was calculated as a percentage of the calcein AM positive cells to the total number of cells.

Reverse transcription-quantitative PCR (RT-qPCR). The 3D and 2D cultured IDG-CM6 cells were incubated in 24-well plates at a density of 2x10^5 cells/well in differentiation medium at 37˚C with 5% CO_2. After 0 and 7 days of differentiation, total RNA of the cells was isolated with a MiniBEST Universal RNA extraction kit (Takara Biotechnology Co., Ltd.) according to the manufacturer's instructions. In addition, after static compressive loading for 6 h, the 3D cultured gel with a density of 2x10^5 cells/gel was ground in liquid nitrogen for 1 min and total RNA was isolated with the same extraction kit. The 3D cultured gel without compressive loading was used as a control. The concentration was calculated by measuring the absorbance at a wavelength of 260 nm using a NanoDrop™ 1000 spectrophotometer (NanoDrop Technologies; Thermo Fisher Scientific, Inc.). A total of 1 mg RNA was used to synthesize complementary DNA with PrimeScript™ RT Reagent kit (Takara Biotechnology Co., Ltd.). The reverse transcription temperature protocol was as follows: 37˚C for 15 min and reverse transcriptase inactivation at 85˚C for 5 sec. RT-qPCR was performed with Applied Biosystems™ 7500 Real-Time PCR system (Thermo Fisher Scientific, Inc.), using SYBR® Premix Ex Taq™ (Takara Biotechnology Co., Ltd.) as a probe. The mRNA levels of mineral metabolic markers, including sclerostin (SOST), osteoprotegerin (OPG), receptor activator of NF-κB ligand (RANKL) and osteocalcin (OCN) were quantified. The thermocycling conditions of the qPCR was as follows: Initial denaturation at 95˚C for 30 sec; followed by 40 cycles of denaturation at 95˚C for 5 sec, annealing at 60˚C for 34 sec and extension at 72˚C for 30 sec. The results were analyzed with the $2^{-\Delta\Delta Cq}$ method to calculate the relative RNA levels, which were normalized to GAPDH (31). The primers were synthesized by Sangon Biotech Co., Ltd., and the primer sequences are listed in Table I.

Statistical analysis. All experiments were repeated in triplicate. The data are presented as the mean ± standard deviation. The statistical analysis was performed using one-way ANOVA followed by Tukey's post hoc test and two-way ANOVA followed by Sidak post hoc test to determine significant differences with SPSS version 19.0 (IBM Corp.). $P<0.05$ was considered to indicate a statistically significant difference.

Results

IDG-CM6 cells exhibit cementocyte-like morphology in both 2D and 3D differentiation conditions. Cementocytes are a type of multi-dendrite cells. The IDG-CM6 cell line is conditionally immortalized with a thermolabile large T antigen, which induces IDG-CM6 cell division (6). Following culture of IDG-CM6 cells in the differentiation conditions, the dendritic processes were increased and extended both in the 2D and 3D differentiation system. On day 28 (Fig. 2A), the canalicular network has been formed by the extending dendrites, which is consistent with the *in vivo* cellular network of cementocytes (5,6). CCK-8 assay was performed to evaluate the proliferation of cementocytes under differentiation conditions in both 2D and 3D groups. In the same differentiation medium, the cells in the 3D system exhibited lower proliferation on day 0 (Fig. 2B; $P<0.05$), however, at day 7, the proliferation of the 3D was faster compared with the 2D group

Table I. List of primers used for reverse transcription quantitative PCR.

Gene	Forward primer (5'-3')	Reverse primer (5'-3')
GAPDH	ATGTGTCCGTCGTGGATCTG	TGAAGTCGCAGGAGACAACC
OPG	ACCCAGAAACTGGTCATCAGC	CTGCAATACACACACTCATCACT
RANKL	CAGCATCGCTCTGTTCCTGTA	CTGCGTTTTCATGGAGTCTCA
SOST	AGCCTTCAGGAATGATGCCAC	CTTTGGCGTCATAGGGATGGT
OCN	CTGACCTCACAGATCCCAAGC	TGGTCTGATAGCTCGTCACAAG

OPG, osteoprotegerin; RANKL, receptor activator of NF-κB ligand; SOST, sclerostin; OCN, osteocalcin.

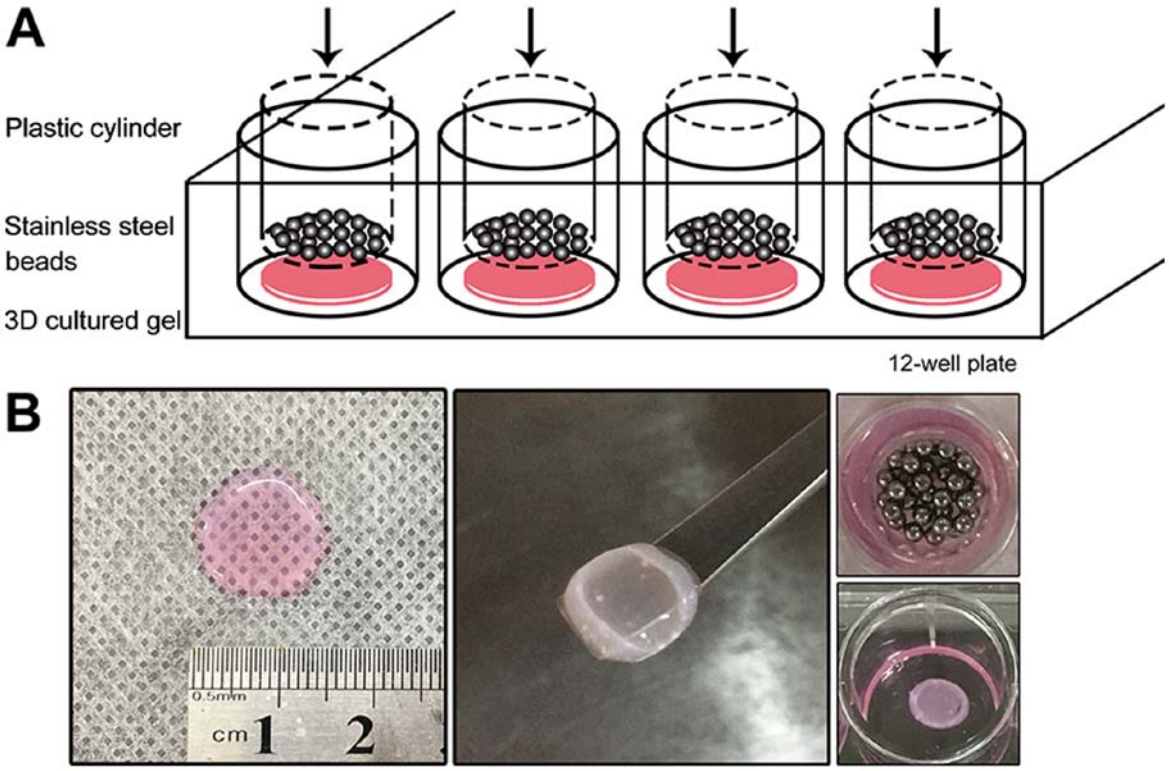

Figure 1. Illustration of the compression loading system. (A) The sterilized stainless-steel beads were added in a plastic cylinder. The cylinder was placed onto the gels. The gravity of the appliances was used to replicate the static compression applied on the cementum. (B) The IDG-CM6 cells were cultured in the 3D scaffolds. Before the compression was applied, the diameter of the gel was measured, and the gel was transferred in a 12-well plate. The force magnitude was adjusted by the number of beads and calculated using the following formula: $P=4m/\pi d^2$. P, pressure; m, total mass of the beads and cylinder; d, diameter; 3D, three-dimensional.

(Fig. 2B; P<0.05). With additional differentiation, cell proliferation declined from day 7 to 35 within each group, and no significance between 2D and 3D group was observed (Fig. 2B).

IDG-CM6 cell line expresses DMP1 and ALP in the 3D scaffold. DMP1 is a marker for cementocytes. The IDG-CM6 cell line has been demonstrated to express DMP1 under differentiation conditions but not immortalized conditions (6). The expression of DMP1 was evaluated via monitoring the expression of GFP, since the IDG-CM6 cell line is derived from the DMP1-GFP$^{+/-}$ mice. GFP expression was not observed in cells cultured in immortalized conditions but in cells in differentiation conditions, starting at day 14 in the 2D group and day 7 in the 3D group (Fig. 3A). Relative fluorescence units of GFP (Fig. 3D) showed that after differentiation for 21 to 35 days, the 3D group expressed higher GFP levels compared with the 2D group (P<0.05). To evaluate the capability of mineral deposition, which is a marker for mineral cell differentiation, ALP staining and ALP activity assay were performed. Decreased expression of ALP was observed in the 3D compared with the 2D group (Fig. 3C), with a significant difference observed at days 5, 7 and 10 (P<0.05). On days 14 and 21, ALP expression peaked and exhibited no significant difference between the groups.

IDG-CM6 cells express OPG, RANKL and SOST mRNA in the 3D differentiation system. OPG, RANKL and SOST are key regulatory cytokines of mechanotransduction, and have been detected in cementocytes (6). The RT-qPCR results of the current study indicated that the cells expressed higher levels of these

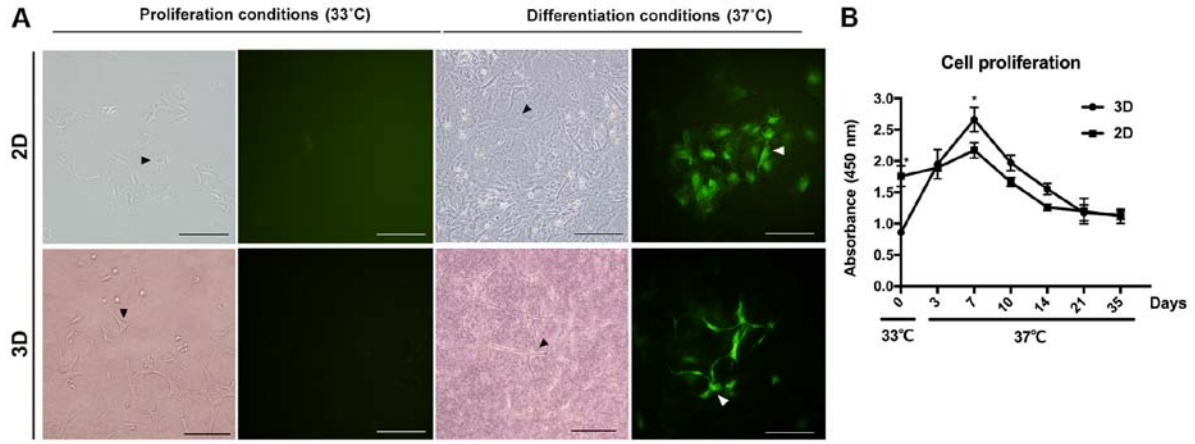

Figure 2. Morphology and GFP expression of the IDG-CM6 cell line. (A) IDG-CM6 cells in proliferation conditions which were multi-dendrite cells without GFP expression, and in differentiation conditions for 28 days where cell clusters formed and high levels of GFP expression (green staining, white arrows) was detected both in the 2D and 3D cultured group. Black arrows indicate IDG-CM6 cells observed under light microscopy. (B) The proliferation rate of IDG-CM6 cells under proliferation (day 0) and differentiation conditions (day 3-35) was detected using Cell Counting Kit-8 assay. The y axis indicates the absorbance at 450 nm. Data are presented as the mean ± standard deviation. *P<0.05, between 2D and 3D groups on days 0 and 7. Scale bars, 20 μm. 2D, two-dimensional; 3D, three-dimensional.

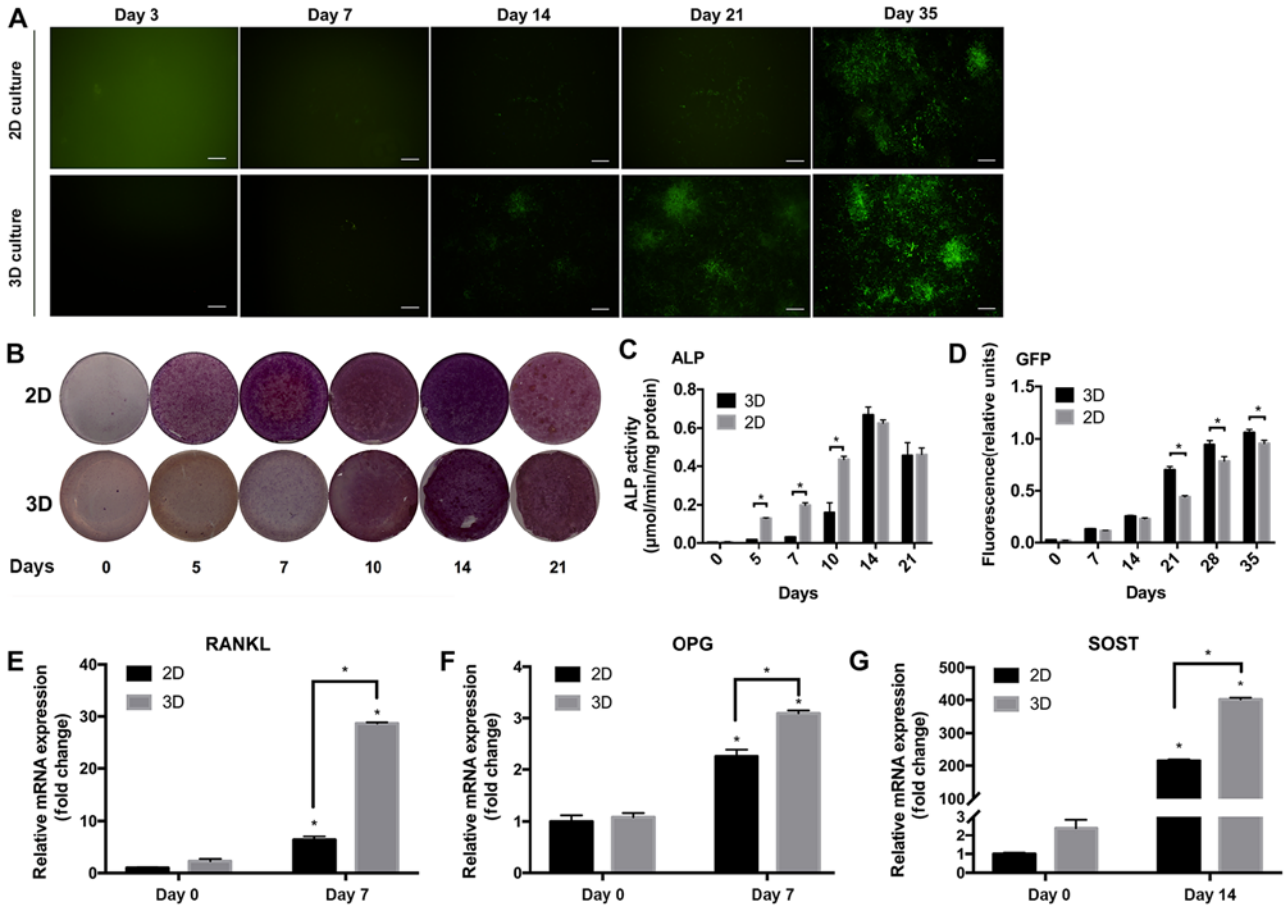

Figure 3. Differentiation of the IDG-CM6 cell line in the 3D scaffold. (A) DMP1-associated GFP expression was detected via fluorescence microscopy and (D) quantified. GFP protein (indicated as green in panel A) was quantified in relative fluorescence units and normalized to the total protein concentration. (B) Alkaline phosphatase activity was detected by ALP staining and (C) quantified in μmol p-nitrophenol phosphate produced per min per mg protein. Relative mRNA expression of (E) RANKL, (F) OPG and (G) SOST genes normalized to GAPDH. The differentiation at 0 and 7 days was compared in the 2D or 3D groups. Data are presented as the mean ± standard deviation. *P<0.05. Scale bars, 20 μm. 2D, two-dimensional; 3D, three-dimensional; GFP, green fluorescent protein; ALP, alkaline phosphatase; RANKL, receptor activator of NF-κB ligand; OPG, osteoprotegerin; SOST, sclerostin; DMP1, dentin matrix protein 1.

markers under 3D differentiation conditions compared with the 2D group or cells without differentiation (P<0.05; Fig. 3E-G).

Static compressive loading indicates that cell viability is magnitude-dependent. The ratio of living cells (stained in

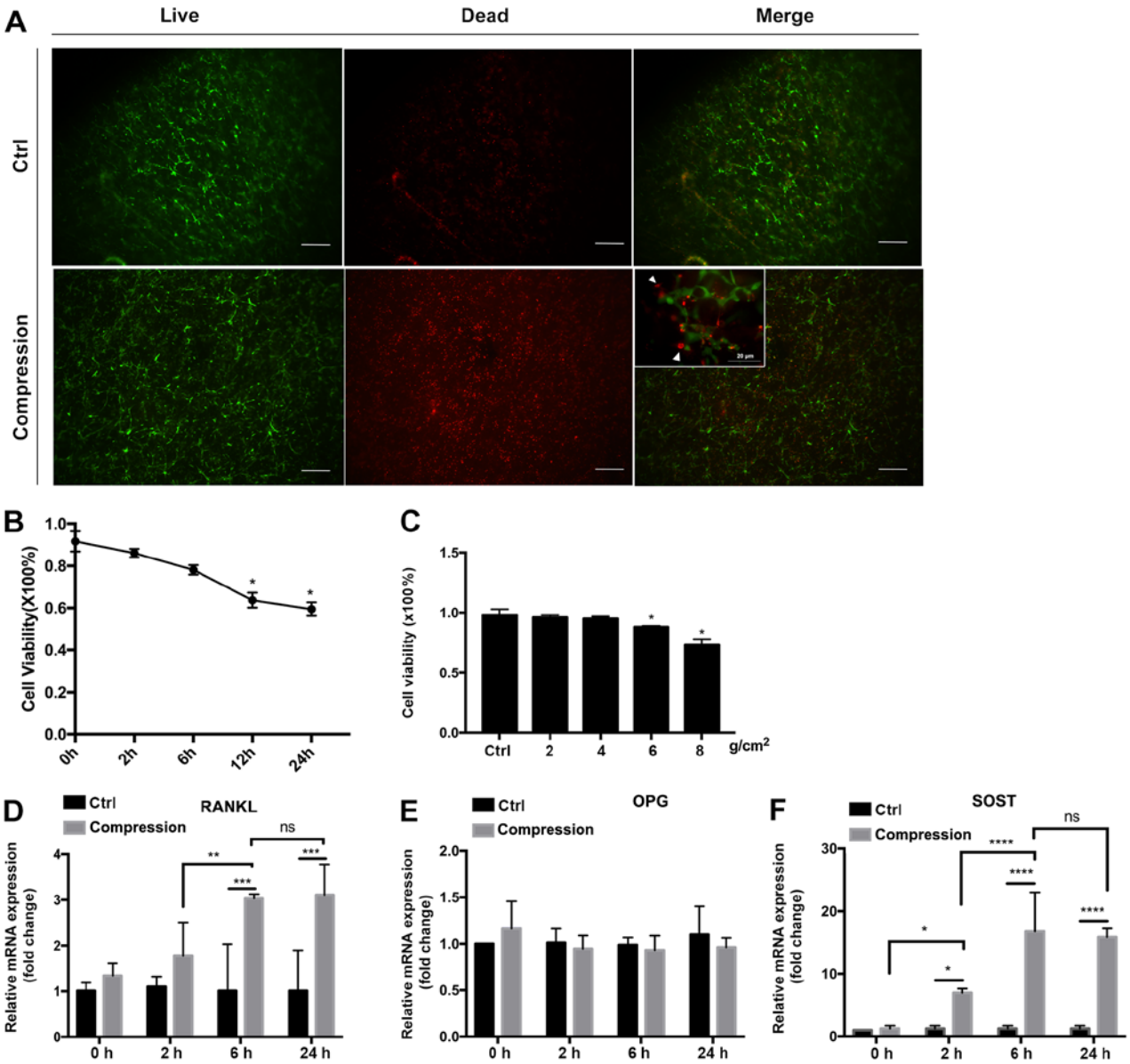

Figure 4. Cell viability and gene expression under static compressive loading. (A) LIVE/DEAD staining at x40 magnification of IDG-CM6 cells under compression of 8 g/cm^2 for 6 h and without compression (Ctrl). Inset, merged images at x400 magnification. Living cells were stained green, while dead cells were stained red (white arrows). The number of red-stained cells was higher in the compression group than in the control group. The numbers of living and dead cells were counted, and the ratio of living vs. dead cells was calculated. (B) Association between the cell viability and force duration when 8 g/cm^2 force was applied. *P<0.05 between each timepoint vs. 0 h. (C) Association of the cell viability with the force magnitude when force was applied for 6 h. *P<0.05 between each magnitude vs. ctrl. (D-F) Relative mRNA expression of (D) RANKL, (E) OPG and (F) SOST normalized to GAPDH in IDG-CM6 cells in response to 8 g/cm^2 force. The mRNA expression was compared between the control and the loading group, and the loading groups were compared relatively to the force duration. Data are presented as the mean ± standard deviation. *P<0.05, **P<0.01, ***P<0.001 and ****P<0.0001. Scale bars, 20 μm. Ctrl, control; ns, not significant; RANKL, receptor activator of NF-κB ligand; OPG, osteoprotegerin; SOST, sclerostin.

green with LIVE/DEAD staining) to total cells (stained in green and red) was calculated to evaluate the cell viability after compression (Fig. 4A-C). A preliminary experiment with 8 g/cm^2 compression force was applied to optimize the treatment time. Cell viability was decreased after 12 h (63.74±3.51%; P<0.05) and 24 h (59.50±3.21%; P<0.05) of compression (Fig. 4B). The expression of SOST (Fig. 4D) and RANKL (Fig. 4F) mRNA increased after 6 h of compression, but additional increase was not detected at 24 h. No significant change in OPG expression (Fig. 4E) was detected at 2, 6 and 24 h of compression. Therefore, 6 h of compression was used for subsequent studies to compare different force magnitudes. Cell viability decreased by values of compressive loading (Fig. 4C), being the lowest in the 8 g/cm^2 force group (72.60±0.08%). No significant differences were observed in the 2 or 4 g/cm^2 force groups, while cell viability was significantly decreased in the 6 and 8 g/cm^2 pressure groups compared with the control group (P<0.05, respectively).

IDG-CM6 upregulates the expression of SOST mRNA and the RANKL/OPG ratio and downregulates OCN in response to compression. SOST is a negative marker of bone formation (32), and the increase of SOST mRNA expression after compression was observed in association with the force magnitude (Fig. 5D),

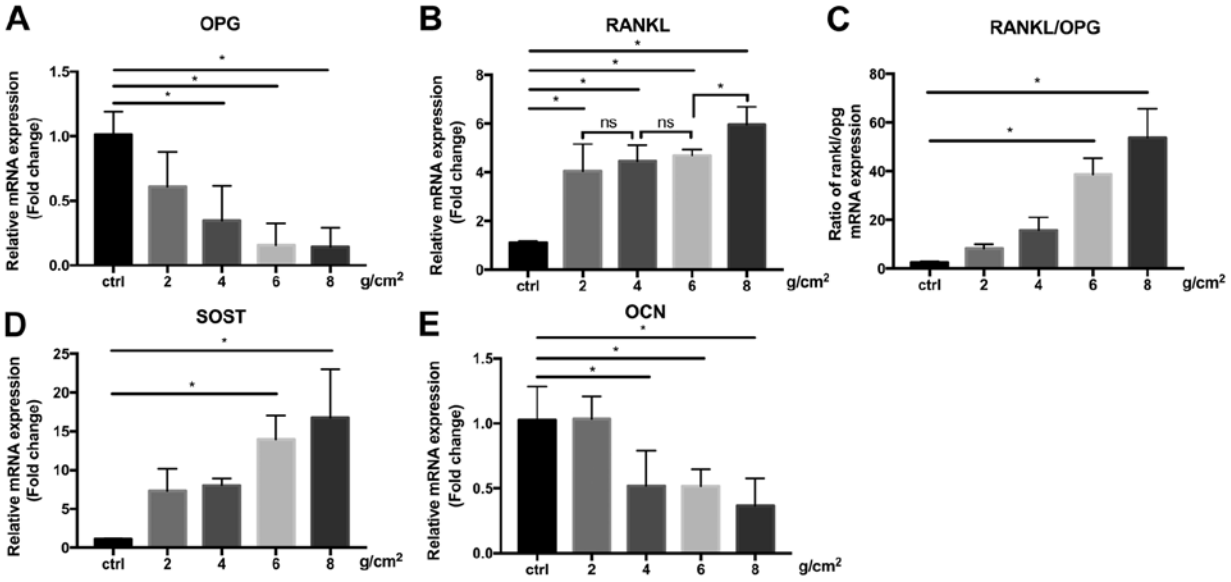

Figure 5. Relative mRNA expression of IDG-CM6 cells when subjected to varying force magnitudes for 6 h. Relative (A) OPG and (B) RANKL mRNA expression normalized to GAPDH. (C) The ratio of RANKL to OPG mRNA expression. (D) Relative SOST and (E) OCN mRNA expression normalized to GAPDH. The values were compared with that of the control group and between different force magnitudes. Data are presented as the mean ± standard deviation. *P<0.05. Ctrl, control; ns, not significant; RANKL, receptor activator of NF-κB ligand; OPG, osteoprotegerin; SOST, sclerostin, OCN, osteocalcin.

with 8 g/cm^2 force inducing the highest increase in SOST expression (16.76±6.26 fold-change vs. GAPDH). RANKL expression was also significantly increased under 2, 4, 6 and 8 g/cm^2 force, however differences between the force magnitudes were only observed between 6 and 8 g/cm^2(P<0.05), but not between 2, 4 and 6 g/cm^2. (Fig. 5B). IDG-CM6 cells exhibited a decreased OPG expression (Fig. 5A) in a force magnitude-dependent manner, with the lowest expression observed in the 8 g/cm^2 force group (0.14±0.15 fold-change vs. GAPDH). Therefore, the RANKL/OPG ratio (Fig. 5C), which is a marker of bone remodeling during orthodontic tooth movement (33), was significantly increased in the 6 and 8 g/cm^2 force groups compared with the control group (P<0.05), and peaked in the 8 g/cm^2 group (53.78±11.86 fold-change vs. GAPDH). OCN is another marker expressed in the cellular cementum and participates in mineral metabolism (5,34). When subjected to compression, a significant decline in OCN expression was observed in the 4, 6, and 8 g/cm^2 (P<0.05) force groups compared with the control group, but not in the 2 g/cm^2 group (Fig. 5E).

Discussion

The current study described the establishment of a 3D cementocyte differentiation model, which may be used to investigate cellular behavior in response to continuous compressive loading. The results indicated that the 3D differentiation system induced mineralized differentiation of the IDG-CM6 cell line and maintained the cementocyte phenotype. The continuous compression on cementocytes was indicated to induce cell death and the expression of osteoclastogenic markers, which has also been observed in other *in vitro* and clinical studies (16,35). The results of the current study suggested that the response of cementocytes to compression loading may be associated with orthodontic-induced tooth root resorption.

Similar to osteocytes, cementocytes are a group of terminally mature cells that are embedded in hard tissues. The terminal differentiation and surrounding minerals represent challenges for studying the function and biological behavior of cementocytes. Previous studies have focused on *in vivo* methods to explore the impact of external stimulation on the cementum, and have revealed that orthodontic forces, inappropriate occlusion and periodontal inflammation lead to osteoclast differentiation and cementum resorption (3,4,16). IDG-CM6 is an immortalized cell line, which reproduces the expression profile of cementocytes observed *in vivo* (36). Zhao *et al* (6) reported that IDG-CM6 presented a different cell behavior in altered culture conditions. In immortalized conditions, the cells have been indicated to exhibit certain features of undifferentiated cells, such as high proliferation and low expression of DMP1, ALP and other mineralization markers (6). On the contrary, the absence of thermo-sensitive T antigen has been demonstrated to induce the cells to express these mineralization markers in differentiation conditions (28). In the present study, IDG-CM6 cells did not express GFP (which was directly associated with DMP1 expression) under proliferation conditions. The results also indicated that when they were transferred in the differentiation conditions (37˚C without IFN-γ), the cells exhibited decreased proliferation, increased expression of DMP1, ALP activity and expression of mineralization regulators, and differentiated into cementocyte-like cells. These results were consistent with a previous study (6). The results of the present study revealed that under the same differentiation conditions, the cells cultured in 3D system expressed a higher level of DMP1, SOST, OPG and RANKL compared with cells cultured in conventional 2D plates. Previous studies have indicated that collagen-based 3D scaffolds facilitated the formation of dendritic processes in mineral cells and replicated the cell network *in vivo* (22,37,38). It has also been reported that the addition of Matrigel to

collagen I maintained the properties of osteocytes and inhibited cell dedifferentiation (26,39). However, to the best of our knowledge, the impact of 3D culture systems on the differentiation of cementocytes has not been reported. In the present study, the lacunar structure of collagen in the 3D culture system may enhance the liquid transfer and the cell network formation, thereby maintaining the cementocyte properties.

DMP1 has been indicated to localize in cementoblasts and cementocytes in human and animal cementum (40,41), acting as a key regulator of the Wnt signaling pathway in mineral metabolism and biomineralization (42). During the formation of the cellular cementum, DMP1 protein has been detected in the pericellular cementum of cementocytes, including their processes, but not in cementoblasts (43). Bae *et al* (44) have reported that the upregulation of DMP1 was associated with the thin and hypomineralized cementum and root dentin of the OC-Cre:Catnb$^{+/lox(ex3)}$ mutant mice, suggesting that DMP1 was involved in the local modulation of the Wnt/β-catenin signaling pathway. In the current study, the cementocytes that were cultured in 3D hydrogel supplemented with differentiation medium, expressed a high level of GFP, which indicated that the cells also expressed a high level of DMP1. In addition, this expression in the 3D model was observed higher than 2D culture at day 21, 28 and 35, indicating a more differentiated cell type.

Increased ALP activity in the 2D culture group compared with 3D culture at days 5, 7 and 10 indicated a delay in the increase of ALP activity in the 3D hydrogel. A marked increase in ALP activity was detected between days 10 and 14. Therefore, the 3D culture system exhibited an equivalent level of ALP expression as that of the 2D culture, indicating a delayed but comparative capacity of mineralization.

Moreover, the 3D system induced the higher expression of SOST, OPG and RANKL genes compared with the 2D system. These markers are expressed by mature cementocytes and act as key cytokines in mechanotransduction and mineral metabolism (45-47). As the cementum is the outmost layer of the tooth root, it withstands the stress from mechanical alterations in the oral environment, such as orthodontic therapies. Therefore, it is possible that the 3D culture system in the present study better represented the physiological conditions of cementocytes and induced IDG-CM6 cells to express a higher level of metabolic genes.

The present study also established a static compression loading system to mimic the orthodontic compression force, which is applied to the tooth root. Sustained orthodontic compression has been indicated to initiate sequential events that cause tooth movement, including the matrix and cell strain, which result in cell activation and differentiation. However, the underlying mechanism remains unclear (48). To explore the cellular response to mechanical loading, efforts have been made to mimic the microenvironment using *in vitro* models, with cyclic and fluid flow shear stress being primarily been used as the loading force (10,12). The compression system of the present study, which utilized gravity to create a static compression force, has been indicated to better mimic the *in vivo* microenvironment (23). The elasticity of the hydrogel has been demonstrated to lead to matrix deformation and strain (26,49), which resemble the *in vivo* matrix strain that is induced by orthodontic forces. The 3D scaffolds have been indicated to embed the cells, and the sparse structure has been revealed to allow the cells to spontaneously form a canalicular network (8,22). In addition, the compression applied to the scaffold has been indicated to prevent direct cell damage compared with the direct forces that are exerted on the monolayer of cells cultured on disks or flasks (16).

The force magnitude and duration time of the compression applied in the current study, which are two factors closely associated with cell and tissue responses, can be adjusted via varying the number of stainless beads and the application time. Therefore, the 3D compression system may be an efficient tool for investigation of the biological processes occurring during orthodontic tooth movement and other mechanotransduction pathways.

During orthodontic tooth movement, the forces that are applied on the teeth are directly and indirectly transferred to the cells surrounding the tooth root (50). Cells that are sensitive to mechanical stress, including osteocytes and PDL cells, respond quickly to the stimulation (51). In the osteocyte-like cell line MLO-Y4, SOST expression has been indicated to decrease under 1 h of compression stress (52), while in human PDL cells, SOST and RANKL expression has been reported to increase in 24 h of compression force (51). The current study applied a heavy force of 8 g/cm^2 to examine the response of the cementocytes to compression, and revealed an increase in SOST and RANKL expression, which was consistent with the previous results on PDL cells. However, compared to the previous study regarding with the PDL cells (51) and osteocytes (52), the response of cementocytes was earlier compared with PDL cells, and comparable to that of the osteocytes, indicating the potential role of cementocytes in early mechanotransduction of tooth movement.

The results of the current study indicated that static compression resulted in increased cell death and expression of osteoclastic markers in cementocytes, while osteogenic markers were inhibited. Moreover, cell viability and the downregulation of OPG and OCN mRNA were indicated to exhibit a force magnitude-dependent pattern, while SOST expression was also associated with the force magnitude. The results of the present study suggested that cementocytes may participate in the modulation of the force-related osteoclast differentiation via the Wnt/β-catenin signaling pathway. These results are consistent with those of previous studies, where animal models have been demonstrated to exhibit root resorption and bone remodeling under compression (53,54). Other *in vitro* studies have also indicated that mechanoreceptor cells, including PDLs and osteocytes, detected forces and activated an intercellular signaling cascade that ultimately results in bone and tooth resorption (11,55,56). However, the results of the current study are in contradiction with a previous study that utilized fluid flow shear stress on cementocytes, which induced an increased cementogenesis differentiation (6). These contradictory results may be attributed to the different type of loading, higher magnitude or longer duration of force employed in these previous studies (6,16,35). Fluid flow shear stress has been considered to increase cell viability, induce well-organized cytoskeleton formation, increase filopodia processes and regulate the osteogenic differentiation of osteocytes (57,58). Different types of force have been reported to induce variable cell responses. The cementoblast-like cell

line OCCM-30 has been indicated to suppress the expression of bone sialoprotein and increase that of osteopontin under 2,000-4,000 microstrain of cyclic stress, and to upregulate microRNA-146b-5p and downregulate SMAD4 under tension (59,60).

Based on previous findings indicating that mild force caused a continuous and constant tooth movement, while heavy force resulted in a periodical and declining tooth movement (50), it can be hypothesized that cementocytes are the potential regulators of compression-induced osteoclast activation, bone resorption and quick tooth movement via regulating the RANKL/OPG ratio, SOST and OCN expression. The cellular response is likely regulated by the magnitude of the force that is applied to the tooth.

The limitations of the current study include the absence of insights into the association between the duration of the force and the cellular response to mechanical loading, which is an important factor in orthodontic therapies. Future studies should explore the cellular crosstalk between cementocytes and adjacent cells such as cementoclasts. Additional studies are required to clarify the mechanism of mechanotransduction and the link between cellular response and tissue remodeling.

In conclusion, the present study established a 3D collagen-based cementocyte model subjected to continuous compressive loading, which simulated the microenvironment of cellular cementum under orthodontic force. The cementocyte-like cell line IDG-CM6 maintained a cementocyte profile in the model and was sensitive to pressure loading in association with the magnitude of force. The present study has revealed that cementocytes possibly function as stress receptors of the tooth in the mechanotransduction process during orthodontic tooth movement. These results expand our knowledge of the biological processes of orthodontic tooth movement and root resorption. This reproducible model is a potential tool for additional studies and for in-depth research on novel therapeutics for tooth movement acceleration.

Acknowledgements

The authors would like to thank Professor Lynda Bonewald (Indiana University, Indianapolis, USA) for the providing cells used in the study and valuable discussions, as well as Dr Xiaolin Wang (Shanghai Jiao Tong University, Shanghai, China) for assistance during the experiments and valuable discussions.

Funding

The current study was funded by National Natural Science Foundation of China (grant nos. 81470765 and 81000420) and the Interdisciplinary Program of Shanghai Jiao Tong University (grant no. YG2016MS06).

Availability of data and materials

The datasets used and/or analyzed during the current study are available from the corresponding author on reasonable request.

Authors' contributions

TW performed the experiments, analyzed the data and drafted the manuscript. YX contributed to data acquisition and interpretation, and critically revised the manuscript. XW contributed to the statistical analysis and drafted the manuscript. NZ contributed to the conception of the study and interpretation of the data, and critically revised the manuscript. GS contributed to the conception and design of the study, and critically revised the manuscript. All authors have read and approved the final version of the manuscript.

Ethics approval and consent to participate

Not applicable.

Patient consent for publication

Not applicable.

Competing interests

The authors declare that they have no competing interests.

References

1. Pitaru S, Pritzki A, Bar-Kana I, Grosskopf A, Savion N and Narayanan AS: Bone morphogenetic protein 2 induces the expression of cementum attachment protein in human periodontal ligament clones. Connect Tissue Res 43: 257-264, 2002.
2. Feller L, Khammissa G, Thomadakis G, Fourie J and Lemmer J: Apical external root resorption and repair in orthodontic tooth movement: Biological events. Biomed Res Int 2016: 4864195, 2016.
3. Walker SL, Tieu LD and Flores-Mir C: Radiographic comparison of the extent of orthodontically induced external apical root resorption in vital and root-filled teeth: A systematic review. Eur J Orthod 35: 796-802, 2013.
4. Brezniak N and Wasserstein A: Orthodontically induced inflammatory root resorption. Part I: The basic science aspects. Angle Orthod 72: 175-179, 2002.
5. Grzesik WJ, Kuzentsov SA, Uzawa K, Mankani M, Robey PG and Yamauchi M: Normal human cementum-derived cells: Isolation, clonal expansion, and in vitro and in vivo characterization. J Bone Miner Res 13: 1547-1554, 1998.
6. Zhao N, Nociti FH Jr, Duan P, Prideaux M, Zhao H, Foster BL, Somerman MJ and Bonewald LF: Isolation and functional analysis of an immortalized murine cementocyte cell line, IDG-CM6. J Bone Miner Res 31: 430-442, 2016.
7. Redlich M, Roos H, Reichenberg E, Zaks B, Grosskop A, Bar Kana I, Pitaru S and Palmon A: The effect of centrifugal force on mRNA levels of collagenase, collagen type-I, tissue inhibitors of metalloproteinases and beta-actin in cultured human periodontal ligament fibroblasts. J Periodontal Res 39: 27-32, 2004.
8. Sun Q, Gu Y, Zhang W, Dziopa L, Zilberberg J and Lee W: Ex vivo 3D osteocyte network construction with primary murine bone cells. Bone Res 3: 15026, 2015.
9. Verbruggen SW, Vaughan TJ and McNamara LM: Fluid flow in the osteocyte mechanical environment: A fluid-structure interaction approach. Biomech Model Mechanobiol 13: 85-97, 2014.
10. Li S, Li F, Zou S, Zhang L and Bai Y: PTH1R signalling regulates the mechanotransduction process of cementoblasts under cyclic tensile stress. Eur J Orthod 40: 537-543, 2018.
11. Manokawinchoke J, Limjeerajarus N, Limjeerajarus C, Sastravaha P, Everts V and Pavasant P: Mechanical force-induced TGFB1 increases expression of SOST/POSTN by hPDL cells. J Dent Res 94: 983-989, 2015.
12. Nieponice A, Maul TM, Cumer JM, Soletti L and Vorp DA: Mechanical stimulation induces morphological and phenotypic changes in bone marrow-derived progenitor cells within a three-dimensional fibrin matrix. J Biomed Mater Res A 81: 523-530, 2007.

13. Atkins GJ, Welldon KJ, Holding CA, Haynes DR, Howie DW and Findlay DM: The induction of a catabolic phenotype in human primary osteoblasts and osteocytes by polyethylene particles. Biomaterials 30: 3672-3681, 2009.
14. Diercke K, König A, Kohl A, Lux CJ and Erber R: Human primary cementoblasts respond to combined IL-1beta stimulation and compression with an impaired BSP and CEMP-1 expression. Eur J Cell Biol 91: 402-412, 2012.
15. Damaraju S, Matyas JR, Rancourt DE and Duncan NA: The effect of mechanical stimulation on mineralization in differentiating osteoblasts in collagen-I scaffolds. Tissue Eng Part A 20: 3142-3153, 2014.
16. Diercke K, Kohl A, Lux CJ and Erber R: Compression of human primary cementoblasts leads to apoptosis: A possible cause of dental root resorption? J Orofac Orthop 75: 430-445, 2014.
17. Tripuwabhrut P, Mustafa K, Brudvik P and Mustafa M: Initial responses of osteoblasts derived from human alveolar bone to various compressive forces. Eur J Oral Sci 120 : 311-318, 2012.
18. Boukhechba F, Balaguer T, Michiels JF, Ackermann K, Quincey D, Bouler JM, Carle GF and Rochet N: Human primary osteocyte differentiation in a 3D culture system. J Bone Miner Res 24: 1927-1935, 2009.
19. Vazquez M, Evans BA, Riccardi D, Evans SL, Ralphs JR, Dillingham CM and Mason DJ: A new method to investigate how mechanical loading of osteocytes controls osteoblasts. Front Endocrinol (Lausanne) 5: 208, 2014.
20. Jagodzinski M, Breitbart A, Wehmeier M, Hesse E, Haasper C, Krettek C, Zeichen J and Hankemeier S: Influence of perfusion and cyclic compression on proliferation and differentiation of bone marrow stromal cells in 3-dimensional culture. J Biomech 41: 1885-1891, 2008.
21. Yamamoto M, Kawashima N, Takashino N, Koizumi Y, Takimoto K, Suzuki N, Saito M and Suda H: Three-dimensional spheroid culture promotes odonto/osteoblastic differentiation of dental pulp cells. Arch Oral Biol 59: 310-317, 2014.
22. Sun Q, Choudhary S, Mannion C, Kissin Y, Zilberberg J and Lee WY: Ex vivo replication of phenotypic functions of osteocytes through biomimetic 3D bone tissue construction. Bone 106: 148-155, 2018.
23. Coyac BR, Chicatun F, Hoac B, Nelea V, Chaussain C, Nazhat SN and McKee MD: Mineralization of dense collagen hydrogel scaffolds by human pulp cells. J Dent Res 92: 648-654, 2013.
24. Ahearne M: Introduction to cell-hydrogel mechanosensing. Interface Focus 4: 20130038, 2014.
25. Damaraju S, Matyas JR, Rancourt DE and Duncan NA: The role of gap junctions and mechanical loading on mineral formation in a collagen-I scaffold seeded with osteoprogenitor cells. Tissue Eng Part A 21: 1720-1732, 2015.
26. Honma M, Ikebuchi Y, Kariya Y and Suzuki H: Establishment of optimized in vitro assay methods for evaluating osteocyte functions. J Bone Miner Metab 33: 73-84, 2015.
27. Fusenig NE, Breitkreutz D, Dzarlieva RT, Boukamp P, Bohnert A and Tilgen W: Growth and differentiation characteristics of transformed keratinocytes from mouse and human skin in vitro and in vivo. J Invest Dermatol 81 (Suppl 1): S168-S175, 1983.
28. Woo M, Rosser J, Dusevich V, Kalajzic I and Bonewald F: Cell line IDG-SW3 replicates osteoblast-to-late-osteocyte differentiation in vitro and accelerates bone formation in vivo. J Bone Miner Res 26: 2634-2646, 2011.
29. Kalajzic I, Braut A, Guo D, Jiang X, Kronenberg MS, Mina M, Harris MA, Harris SE and Rowe DW: Dentin matrix protein 1 expression during osteoblastic differentiation, generation of an osteocyte GFP-transgene. Bone 35: 74-82, 2004.
30. Tawakoli PN, Al-Ahmad A, Hoth-Hannig W, Hannig M and Hannig C: Comparison of different live/dead stainings for detection and quantification of adherent microorganisms in the initial oral biofilm. Clin Oral Investig 17: 841-850, 2013.
31. Livak KJ and Schmittgen TD: Analysis of relative gene expression data using real-time quantitative PCR and the 2(-Delta Delta C(T)) method. Methods 25: 402-408, 2001.
32. Tu X, Rhee Y, Condon KW, Bivi N, Allen MR, Dwyer D, Stolina M, Turner CH, Robling AG, Plotkin LI and Bellido T: Sost downregulation and local Wnt signaling are required for the osteogenic response to mechanical loading. Bone 50: 209-217, 2012.
33. Silva I and Branco JC: Rank/RANKL/OPG: Literature review. Acta Reumatol Port 36: 209-218, 2011.
34. García-Martín A, Reyes-García R, Avila-Rubio V and Muñoz-Torres M: Osteocalcin: A link between bone homeostasis and energy metabolism. Endocrinol Nutr 60: 260-263, 2013 (In English, Spanish).
35. Matsuzawa H, Toriya N, Nakao Y, Konno-Nagasaka M, Arakawa T, Okayama M and Mizoguchi I: Cementocyte cell death occurs in rat cellular cementum during orthodontic tooth movement. Angle Orthod 87: 416-422, 2017.
36. Wang H, Li T, Wang X, Yin X, Zhao N, Zou S, Duan P and Bonewald L: The role of sphingosine-1-phosphate signaling pathway in cementocyte mechanotransduction. Biochem Biophys Res Commun 523: 595-601, 2020.
37. Pedraza CE, Marelli B, Chicatun F, McKee MD and Nazhat SN: An in vitro assessment of a cell-containing collagenous extracellular matrix-like scaffold for bone tissue engineering. Tissue Eng Part A 16: 781-793, 2010.
38. Uchihashi K, Aoki S, Matsunobu A and Toda S: Osteoblast migration into type I collagen gel and differentiation to osteocyte-like cells within a self-produced mineralized matrix: A novel system for analyzing differentiation from osteoblast to osteocyte. Bone 52: 102-110, 2013.
39. Dewitt DD, Kaszuba SN, Thompson DM and Stegemann JP: Collagen I-matrigel scaffolds for enhanced Schwann cell survival and control of three-dimensional cell morphology. Tissue Eng Part A 15: 2785-2793, 2009.
40. Bosshardt DD: Are cementoblasts a subpopulation of osteoblasts or a unique phenotype? J Dent Res 84: 390-406, 2005.
41. Sawada T, Ishikawa T, Shintani S and Yanagisawa T: Ultrastructural immunolocalization of dentin matrix protein 1 on Sharpey's fibers in monkey tooth cementum. Biotech Histochem 87: 360-365, 2012.
42. Bonewald LF: The amazing osteocyte. J Bone Miner Res 26: 229-238, 2011.
43. Toyosawa S, Okabayashi K, Komori T and Ijuhin N: mRNA expression and protein localization of dentin matrix protein 1 during dental root formation. Bone 34: 124-133, 2004.
44. Bae CH, Lee JY, Kim TH, Baek JA, Lee JC, Yang X, Taketo MM, Jiang R and Cho ES: Excessive Wnt/β-catenin signaling disturbs tooth-root formation. J Periodont Res 48: 405-410, 2013.
45. Lehnen SD, Gotz W, Baxmann M and Jager A: Immunohistochemical evidence for sclerostin during cementogenesis in mice. Ann Anat 194: 415-421, 2012.
46. Boyce BF and Xing L: Functions of RANKL/RANK/OPG in bone modeling and remodeling. Arch Biochem Biophys 473: 139-146, 2008.
47. Jäger A, Götz W, Lossdörfer S and Rath-Deschner B: Localization of SOST/sclerostin in cementocytes in vivo and in mineralizing periodontal ligament cells in vitro. J Periodontal Res 45: 246-254, 2010.
48. Li Y, Jacox LA, Little SH and Ko CC: Orthodontic tooth movement: The biology and clinical implications. Kaohsiung J Med Sci 34: 207-214, 2018.
49. Taki M, Yamashita T, Yatabe K and Vogel V: Mechano-chromic protein-polymer hybrid hydrogel to visualize mechanical strain. Soft Matter 15: 9388-9393, 2019.
50. Krishnan V and Davidovitch Z: Cellular, molecular, and tissue-level reactions to orthodontic force. Am J Orthod Dentofacial Orthop 129: 469.e1-e32, 2006.
51. Odagaki N, Ishihara Y, Wang Z, Ei Hsu Hlaing, Nakamura E, Hoshijima M, Hayano M, Kawanabe S and Kamioka N: Role of osteocyte-PDL crosstalk in tooth movement via SOST/Sclerostin. J Dent Res 97: 1374-1382, 2018.
52. Shu R, Bai D, Sheu T, He Y, Yang X, Xue C, He Y, Zhao M and Han X: Sclerostin promotes bone remodeling in the process of tooth movement. PLoS One 12: e0167312, 2017.
53. Gonzales C, Hotokezaka H, Yoshimatsu M, Yozgatian JH, Darendeliler MA and Yoshida N: Force magnitude and duration effects on amount of tooth movement and root resorption in the rat molar. Angle Orthod 78: 502-509, 2008.
54. Chen L, Mo S and Hua Y: Compressive force-induced autophagy in periodontal ligament cells downregulates osteoclastogenesis during tooth movement. J Periodontol 90: 1170-1181, 2019.
55. Bumann EE and Frazier-Bowers SA: A new cyte in orthodontics: Osteocytes in tooth movement. Orthod Craniofac Res 20 (Suppl 1): S125-S128, 2017.
56. Murshid SA: The role of osteocytes during experimental orthodontic tooth movement: A review. Arch Oral Biol 73: 25-33, 2017.

57. Yan Z, Wang P, Wu J, Feng X, Cai J, Zhai M, Li J, Liu X, Jiang M, Luo E and Jing D: Fluid shear stress improves morphology, cytoskeleton architecture, viability, and regulates cytokine expression in a time-dependent manner in MLO-Y4 cells. Cell Biol Int 42: 1410-1422, 2018.
58. Ajubi NE, Klein-Nulend J, Nijweide PJ, Vrijheid-Lammers T, Alblas MJ and Burger EH: Pulsating fluid flow increases prostaglandin production by cultured chicken osteocytes-a cytoskeleton-dependent process. Biochem Biophys Res Commun 225: 62-68, 1996.
59. Huang L, Meng Y, Ren A, Han X, Bai D and Bao L: Response of cementoblast-like cells to mechanical tensile or compressive stress at physiological levels in vitro. Mol Biol Rep 36: 1741-1748, 2009.
60. Wang L, Hu H, Cheng Y, Chen J, Bao C, Zou S and Wu G: Screening the expression changes in MicroRNAs and their target genes in mature cementoblasts stimulated with cyclic tensile stress. Int J Mol Sci 17: 2024, 2016.